FIBRE ROPE MODELLER (FRM) : A CAD program for the Performance Prediction of Advanced Cords and Ropes under Complex Loading Environments.

S. Banfield, J.W.S. Hearle, C. M. Leech, [Tension Technology International], R.Tebay, and C.A.Lawrence [University of Leeds]

ABSTRACT

Two factors are driving advances in synthetic fibre yarns, cords and rope technology. The first is the development and exploration of first and second generation synthetic fibres and the introduction of new rope constructions that offer the potential for major improvements in rope properties. The second is the growing range of synthetic fibre engineering applications being studied. A number of major ventures have already been brought to realisation. For example, the US Navy interest in mooring a large “air-base” in deep water in the Pacific and the exploitation of oil fields in greater water depths (500 – 3000m) makes light weight fibre ropes an attractive practical alternative to wire ropes or chains. Fibre structures are also replacing steel wire structures in some other traditional uses and have the potential for important advances in tyre cords, medical ligaments, bridges, textile architectural buildings, towed arrays, space structures and other engineering applications.

Polymeric fibres have complex mechanical properties and fibre structures can be geometrically complex involving interactions between millions of fine fibres. These features lead to the major difficulty of predicting fibre structure performance when subjected to complex loading over long periods of time. As a result the traditional practice for structural engineers is to use designs based on practical experience. In contrast to steel wire ropes which operate in the linear elastic range, fibre structures have non-linear, inelastic and visco-elastic properties, partly resulting from the organic polymeric materials used to make them and partly from friction between fibres and the compacting of the structure. Modelling of the performance of synthetic structures is therefore a necessary step in the design life prediction of new fibre products for engineering applications. The provision of CAD software is therefore essential to the future competitiveness of synthetic structure manufacturers, consultants and structural engineers.

This paper describes and demonstrates FRM developed for the design and performance prediction of yarns, cords and ropes for complex loading in marine, civil and aerospace applications. FRM is modular in form. The two basic modules cover the synthetic structure construction and tension, torque, elongation and twist response. Other modules cover fatigue effects. The geometry is hierarchical, through the levels of structure in a rope :e.g. filament, textile yarn, rope yarn, strand, rope. Strains are determined from imposed deformations. External and internal forces are computed by the principle of virtual work. Fatigue effects are computed, in sequence, for single cycles and then extrapolated for many cycles before re-computing. The information presented will be of interest to oil, engineering, civil and aerospace companies as there is now a growing need to employ more computer and IT techniques in the design and development of new products.

MODELLING PRINCIPLES

Rope geometry and fibre content

The modelling of structure geometry follows a hierarchical approach with a number of levels, which mirrors the manufacturing process. Typical sequences are filament, textile yarn, ropeyarn, strand, sub-rope, rope and some typical rope constructions are illustrated in Fig. 1. These are specified in terms of: linear density (mass/length); density, which determines diameter and depends on fibre density and packing factor within the yarns; tensile stress-strain properties; and coefficient of friction. Different fibres may be combined within the same rope.

At each structural level (e.g., a strand), the next lower level form (e.g., the rope yarn) follows a uniform helical path around a central axis as shown in Fig. 2. This means that an individual filament will follow a complicated path determined by the multiplicity of helices. However, since the properties of each level are determined separately and used as input to the next higher level, these complications are avoided and the only geometry that needs to be defined is that of Fig. 2, with

relations derived from the triangles in the "opened-out" diagram. The consequences on twist at a lower level of the subsequent twisting at a higher level have to be taken into account.

Packing involves both qualitative and quantitative aspects. Three forms of arrangement of components, shown in Fig. 3, are considered: in "packing" geometry, the elements are in circular layers where the contact stresses act radially towards the central axis; in "wire-rope" geometry, circular layers are self-supported by circumferential pressures where contact stresses act circumferentially within the assembly; in "wedge" geometry the components are deformed into pieces bound by segments of radii and arcs, and generate contact forces both radially and circumferentially. For each geometry, there is a packing factor in the stress-free state, which may be reduced by lateral pressures developed under tension.

Variability in structure and fibre properties may have an appreciable influence on rope strength, especially in low twist highly lubricated ropes.

Rope deformation

The basic deformation assumption is that planes perpendicular to the axis of the helical structure within each component remain planar and perpendicular to that axis. The circular cross-sections at either end of the element in Fig. 2 thus move farther apart due to extension, rotate relative to one another due to twist, and reduce in area either to keep the volume constant or to allow for compression. Analysis by differential geometry then gives expressions for the elongation of the lower level components, and keeps track of the sequence of imposed deformations through the several layers of the structure.

In order to introduce frictional effects, it is necessary to consider slip at contact points. The modes of slip are numerous, and their magnitude must be found from the differential geometry of deformation. Those identified as the more important and taken into account as appropriate, particularly in the later fatigue studies, are illustrated in Fig. 4 and listed as follows: modes 1 and 2, axial sliding between components due to stretching and twisting of the structure; mode 3, rotational slip, which is an end-effect; mode 4, scissoring at crossovers; mode 5, sawing at crossovers; mode 6, bulk compression or dilation. There is also component distortion, which has not yet been explicitly treated, but is implicitly catered for by providing treatments for both the initial, cylindrical, and final, wedge, shaped construction geometries. The scissoring, sawing and bulk compression modes of slip have been identified as significant in fatigue failure mechanisms but not in their effect on rope loads, as they are associated with small displacements.

Rope mechanics

The analysis is based on the Principle of Virtual Work:

$$\mathbf{P}*\mathbf{L} + \mathbf{T}*\mathrm{N} = *\mathbf{U}$$

where **P** is tension and **L** is elongation, **T** is torque and N is twist, and **U** is strain energy.
Because the rope is composed of an extremely large number of fine filaments, bending and torsional effects in the input components can be neglected. It is only necessary to take account of elongation energy obtained by integration of the tensile stress-strain properties, which can be measured on yarns in extension and recovery. Effects at higher levels come naturally into the analysis.

Application of virtual displacements then gives the expressions for tension and torque:

$$\mathbf{P} = 3\Phi_c\mathbf{l}_{oc}(*\gamma_c/*\mathbf{L}) \quad \mathbf{T} = 3\Phi_c\mathbf{l}_{oc}(*\gamma_c/*\mathrm{N})$$

where Φ_c is the axial load in the component as a function of $\Phi_c(\mathbf{L},\mathrm{N})$, $\mathbf{l}_{oc}$ is the reference length of the component, and γ_c is the strain in the component.

In order to determine contact forces between components in the structure, it is necessary to introduce a virtual change in the helix radius **a**. The contact force per unit length is then given by expressions similar to the above involving $(\gamma_c/*\mathbf{a})$. The frictional force is given by multiplying the contact force by the coefficient of friction. The frictional contribution to the deformation energy, which must be added

into the computed work, is the product of friction force and displacement at the contacts as derived from the rope deformation. The only significant contribution, and even that is small, comes from the axial sliding mode.

The analysis outlined above enables tension and torque in ropes to be calculated as functions of elongation and twist. Breakage occurs when the input components, normally yarns, reach their breaking extension. Except in unusual constructions, this will indicate the maximum load, namely the rope strength, and, in practice, will usually be the trigger for catastrophic failure.

FATIGUE MODELLING

Basic technique

The quasi-static rope modelling, described by Leech, Hearle, Overington and Banfield, (1993) and embodied in computer software in its own right, leads to predictions of the response of rope to a cycle of extension and recovery. In principle the software can handle all levels of components in a rope: e.g., filaments, "textile" yarns, rope yarns, strands, and sub-ropes. In practice, either textile or rope yarns are taken as the basic level. The information generated includes the tensile forces on all components, the contact pressures between components, the relative slip of components, and the energy dissipated as heat.

The basic principle of fatigue modelling is that the changes in material properties, as a result of the cyclic loading, can be determined and used as the input for the rope response in the next cycle. It would take too much computer time to compute the response in every cycle of a long lifetime of use. The scheme adopted therefore computes the response for a selected cycle, finds the resulting increment of fatigue, assumes that the same effect occurs in successive cycles, and then, after a selected interval, updates the model and computes the response in another cycle. At the start and finish of the lifetime, when large changes are occurring, the intervals may be short, possibly even computing each cycle, but in the middle range, where minimal changes may be occurring, they might be very long.

It is now necessary to consider how each of the three modes is brought into the software.

Creep rupture

The work of Meredith (1954), which has been confirmed by later studies, shows that the strength **S** of fibres falls logarithmically with time **t** under load according to the equation:

$$\mathbf{S} = \mathbf{S}_g [1 - \mathbf{k} \log(\mathbf{t}/\mathbf{t}_g)] \quad \text{.....(1)}$$

where $\mathbf{S}_g$ and $\mathbf{t}_g$ are the strength and time for known test conditions and **k** is the strength-time coefficient.

Within experimental error, this equation applies whether the time relates to a period under constant load **S**, to a period of cyclic loading to a maximum load **S**, or to an increase to a break load **S** in a tensile test. It is worth noting the major influence of the value of the strength-time coefficient, as shown by Table 1. There is good experimental data showing that for nylon **k** = 0.08, which makes creep failure a significant problem. It is much less serious with polyester and aramid ropes, where **k** is just above and just below 0.05 respectively, but is even more serious with polyethylene (including some HMPE) where **k** is nearer 0.2.

k	time to fail at per cent of 1 minute break load			
	20%	50%	65%	80%
0.05	2×10^{10} years	200,000 years	20 years	200 hours
0.1	200 years	60 days	5 hours	100 minutes
0.2	8 days	5 hours	1 hour	10 minutes

The above equation can be used directly to obtain a rough estimate of the time-to-break of ropes under load. However better estimates, and in particular the interaction with other modes of failure, which changes the load on components, require a more detailed procedure.

The input data from tests on yarns, or the accumulated experience on each fibre type, relates the tension to the time-to-break. A set of modified load-extension curves is then established for a range of times $\mathbf{t}_u$ by changing the break load according to equation (1) and scaling the rest of the curve by the same factor, thus leaving the polynomial coefficients defining the shape of the load-elongation curves unchanged.

For regular cycling to peak load **P** with a frequency **f**, the time **t** in one cycle is 1/**f**. For the first cycle, the load-elongation curve for $\mathbf{t}_u = \mathbf{t}$ is selected and run in extension and recovery. This is then assumed to approximate the response for a total of (**N**-1) cycles. For the **N**th cycle, the load-elongation curve is changed to that for $\mathbf{t}_u = \mathbf{Nt}$ and the cycle of extension and recovery is run again. This procedure is repeated for successive numbers of cycles. Fibre breakage is introduced by checking the loads on components. If any elements experience a peak load greater than their break load adjusted for elapsed time, their contribution is reduced to zero. This effectively increases the stress on the remaining elements.

Hysteresis heating

As described by Leech, Hearle, Overington and Banfield, (1993), the computer code provides values for the heat generation due to fibre hysteresis and frictional losses and also uses a summation of the heat flow from different sources to compute the temperature changes. As an example, Fig. 5 shows how heat sources would be distributed in a three-strand rope.

The change in temperature alters the load-elongation properties of the yarns, and so the input to the program must be updated at intervals of cycles in order to allow for this. The exact procedure adopted will depend on the nature of the experimental evidence on change of fibre properties with temperature. It is usually appropriate to introduce linear variations of break load and extension with temperature, and leave the polynomial coefficients unchanged.

For marine use, it is assumed that the rope surface temperature is equal to that of the water and that all spaces within the rope are flooded. It is worth noting that excessive heating can be avoided by replacing a large rope with an equivalent number of small ones. In these circumstances, the program is a valuable design tool, rather than a predictor of performance of a deployed installation. For use in air, it would be necessary to extend the program to include heat transfer from the rope surface.

Internal abrasion

Internal abrasion has been shown to be a dominant cause of failure of highly structured nylon ropes under mild loading conditions. In one test [OCIMF Hawser Test Report, 1982], a braided nylon rope cycled wet to 50% of its break load failed in less than 1000 cycles. In low-twist polyester and aramid ropes, internal abrasion in tension-tension fatigue at low loads is not a problem. For higher twist polyester and aramid ropes, internal abrasion at moderate to high loads can be a problem. The theory and computing of internal wear in ropes is the most complicated so far attempted. In addition, as discussed later, the experimental data on fibre properties is not easily available. However the development of a model provides an incentive for more detailed work, probably in response to some particular engineering demand. There is a synergistic benefit in linking theoretical modelling with practical investigations.

Internal abrasion results from the relative displacement (slip) of fibres in contact under normal loads (transverse stresses). The frictional forces generate shear stresses within the fibres, and these cause cracks to develop and propagate, with eventual complete fibre breakdown. In principle, the damage is controlled by the magnitude of the computed normal loads and slip.

In order to compute the effects of wear, we introduce a rate of wear parameter **F**, equal to the fraction of fibre lost per cycle under the conditions existing at the contact. In **N** cycles, a total of **NF** fibres will be lost at the contact. In general **F** will be a function of: contact pressure; coefficient of friction;

magnitude of slip; contact geometry and slip direction; environment (temperature, moisture etc); rate of slip; presence of debris; and possibly other factors.

All the significant contacts between components (strands, yarns, filaments) are considered. In one cycle, the extent of wear in each component is computed under the loading conditions experienced by the particular component as determined by the software, and then multiplied for a sequence of **N** cycles. The lost fibres are assumed to cease to contribute tensile forces in the rope, but to continue to fill space and transmit transverse forces. The rope geometry is not altered by the fibre wear.

The repetition of this sequence leads to a progressive reduction in the number of active fibres in the rope, increases the loads on other fibres, and eventually leads to their removal by breakage, taking account of time and temperature effects on fibre strength.

A simpler global version of the treatment of internal abrasion in the program assumes that wear resistance is constant throughout the rope and can be predicted from the total forces on the rope. This is based on two assumptions

(i) wear resistance is constant throughout the rope (no localisation of contact damage points),

(ii) rate of wear depends only on maximum tension or tension range (expressed as a fraction of break load) and does not increase as the stresses in the components increase because of the removal of some material,

and on current experimental data obtained directly from rope fatigue tests, until more specific information on wear is known. The rope fatigue data, which necessarily includes the effects of other fatigue mechanisms, is then an extremely conservative estimate for internal abrasion by itself. The program relates cycles to failure to tensile load range as

$$\text{Log}(\mathbf{N}) = \mathbf{a} + \mathbf{b}\ (\%\ \text{of breaking stress})$$

where **N** is the number of cycles to failure and **a** & **b** are constants for a particular rope construction and its constituent materials.

Real life applications of FRM modelling

A number of measurements (Leech, CM, Hearle, JWS, Overington, MS and Banfield, SJ 1993) of tension and torque developed in ropes, strands and yarns have been performed in order to confirm the validity of the theory and computer codes. Figure 6 shows the good correlation in load/elongation between theory and experiment for all three levels (the rope itself, a sub-rope and a sub-rope strand) of a parallel strand polyester rope.

Fig. 7 presents the predicted fatigue plots of residual strength against Log(time) with different values of the **local abrasion** rate of wear parameter **F**, on a 7 strand aramid rope cycled at wave period (6s or 0.167Hz) between 16% and 45% of its predicted new breaking strength. In all cases the same value of **F** was applied to every contact and the software predicts equilibrium temperatures of 72EC in the core strand and 32EC in the outer strands, so the effect of hysteresis is constant. With **F** = zero the predicted lifetime is almost 202 million cycles and we are predominantly seeing the effects of creep rupture. With **F** increasing through 0.0002, 0.002 and 0.02, which corresponds to a fibre loss in 5000, 500, and 50 cycles, lifetimes decrease rapidly to 1047072, 133981 and 18403 cycles respectively, due to the effects of abrasion.

Fig. 8 presents the predicted fatigue plot of residual strength against log(time) with **global abrasion** parameters (**a** = 10.009 & **b** = -0.107) for a 5 tonne aramid rope cycled at 2Hz between 14% & 42% of its predicted new breaking strength. The progressive reduction of break load takes account of the effects of creep rupture, hysteresis heating and abrasion damage. The experimental point shown depicts the residual strength of a rope which was removed from a test after it had survived 1 million cycles.

VISCOELASTICITY AND STIFFNESS

In most applications of fibre structures, load and deformation vary with time, sometimes intermittently and sometimes periodically. Some actions are elongation driven, for example the vertical displacement of a moored vessel due to wave motion, which determines peak load, and some are force driven, for example wind and wave action.on a vessel, which determines horizontal offset. In both cases the effective stiffness (tension/elongation) of the rope determines the relation between force and elongation. Engineers need to know this stiffness in order to compute the response of a total system, for example in mooring analyses. For an ideal elastic material, stiffness is uniquely given by size and modulus. For fibre structures, it is not so simple, due to the viscoelasticity of the material, frictional slip between components, and bedding-in of the structure. In general, stiffness will depend on mean load, cyclic load range, previous loading history, temperature etc. Fig. 9 is a simple illustration of the differences in stiffness in an aramid rope on initial extension and in cyclic loading at different levels.

The response to any increment or cycle of loading could, in principle be represented by the model shown in Fig. 10, which includes elastic, viscous and frictional elements in series and in parallel, provided the values of the parameters are allowed to change with the loading conditions and history. However, it is too difficult a problem to determine the vast amount of data needed to fully characterise the model, and there is no adequate theory of non-linear viscoelasticity to apply. Current work on FRM is directed to finding ways round this problem. Rope testing is showing how the model can safely be simplified. The mean length of the rope is largely determined by F_1 which relates to bedding-in and V_1, which relates to fibre creep. The cyclic loading response can be approximated by a modulus, effectively lumping all the elastic elements into E_1, with the viscous and frictional elements determining a small loss factor. Successful application of FRM depends on finding a set of yarn tests, which can be used as inputs to the rope model to reflect the material properties in complex loading histories, and empirical relations to allow for rope bedding-in.

CONCLUSION

The analysis of fibre structures outlined in this paper enable worthwhile predictions of the load/strain/torque/fatigue response to be calculated. Tension and torque can be computed in their dependence on elongation and twist, and the breakage of filaments, textile yarn, strands and ropes predicted. Computer modelling of fibre assemblies, cords and ropes will become an essential tool for the designer. Some applications include:

- basic structure design eg parametric studies to improve design
- reduce material costs through improved design
- supplement laboratory testing and reduce test/time costs
- field applications eg predicting static and fatigue properties in actual service

These codes have already been used to design ropes for floating production system mooring studies and to assist ropemakers with new rope designs.

Acknowledgment

The financial support of the DTI and Marlow Ropes into this study is gratefully acknowledged.

References

Hearle, J.W.S., Parsey, M.R., Overington M.S. and Banfield S.J. (1993). "Modelling the Long Term Performance of Fibre Ropes", *Third (1993) International Offshore and Polar Engineering Conference, Singapore*.
Leech, CM, Hearle, JWS, Overington, MS and Banfield, SJ (1993). "Modelling Tension and Torque Properties of Fibre Ropes and Splices", *Third (1993) International Offshore and Polar Engineering Conference, Singapore*.
Meredith, R. (1954) *J. Textile Inst.*, **45**, T30.
OCIMF *(1982) "Hawser Test Report. Data on Large Synthetic Ropes in the Used Condition*".

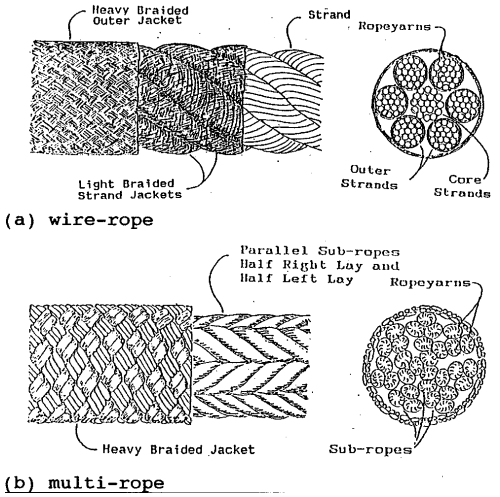

Figure 1.Rope constructions

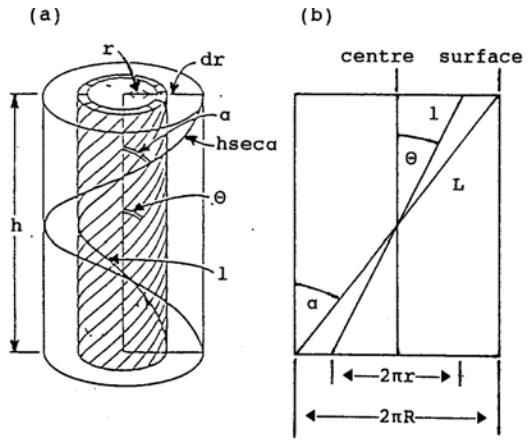

Figure 2.Twist geometry (a) components follow helical paths round concentric cylinders and (b) opening out flat defines geometrical and trigonometrical relations

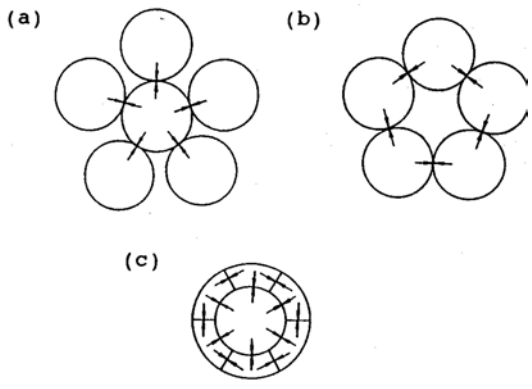

Figure 3. Cross section geometry (a) packing, (b) wire rope, (c) wedge

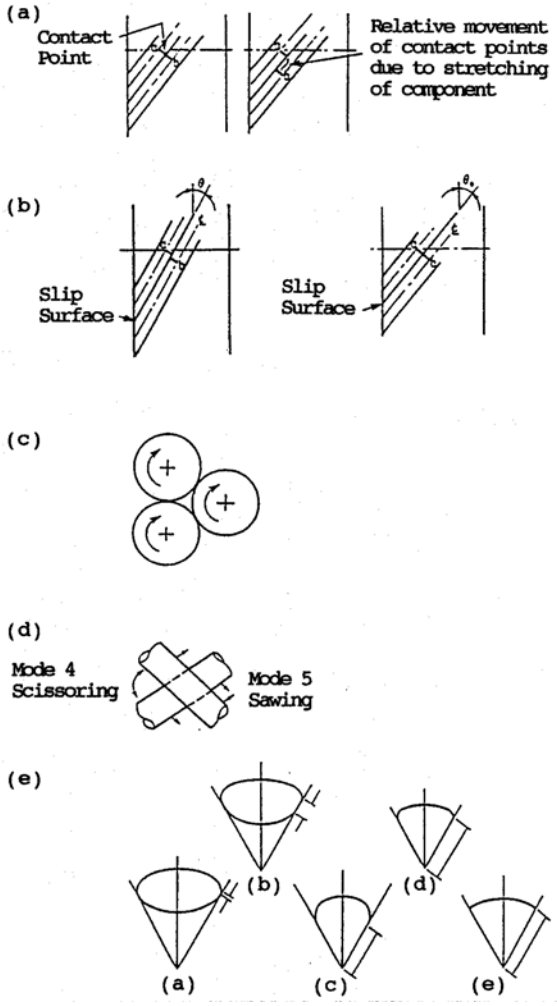

Figure 4. Modes of slip (a) mode 1 stretching, (b) mode 2 twisting, (c) mode 3 rotating, (d) mode 4 scissoring and sawing, (e) mode 6 distortion

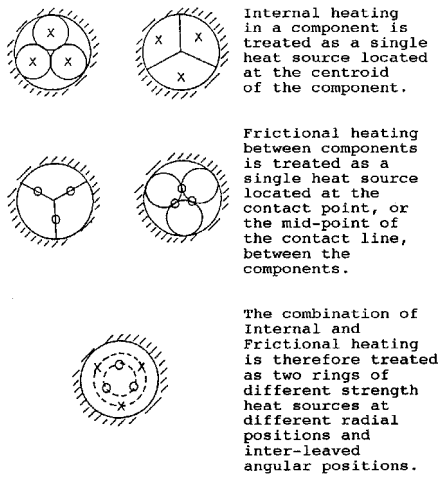

Figure 5 Distributed heat sources in a three strand rope

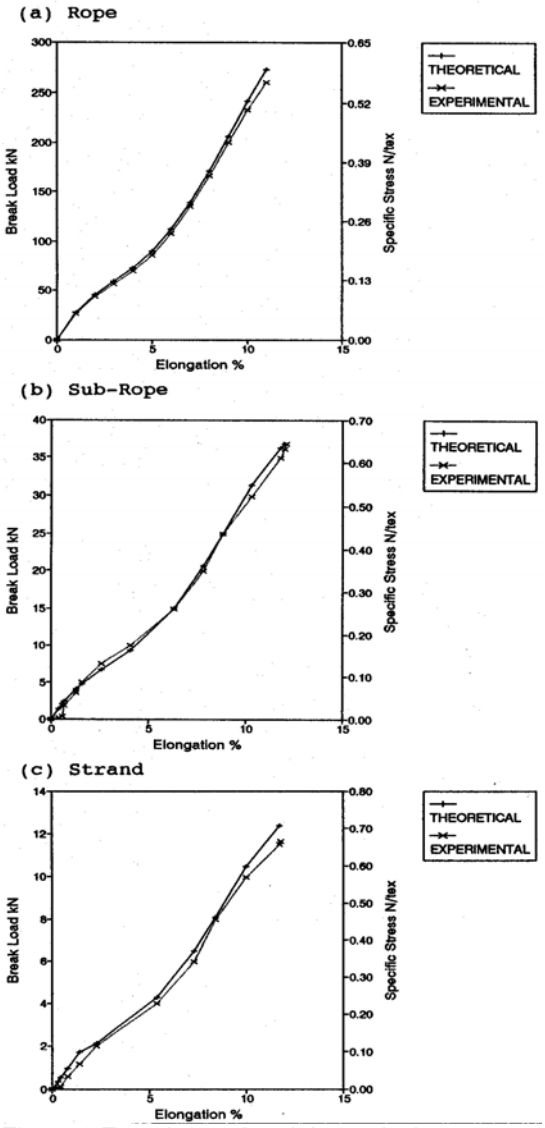

Figure 6.Experimental and theoretical load/elongation curves for parallel strand polyester

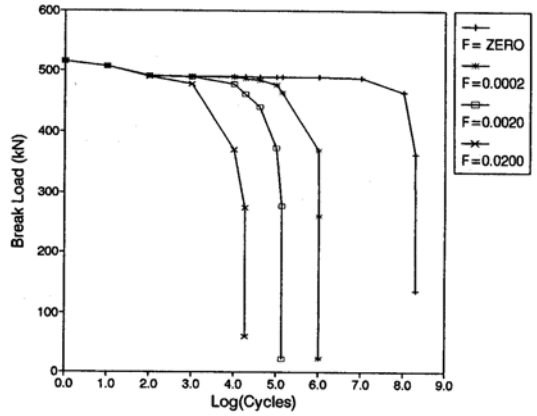

Figure 7 Examples of predicted residual strength throughout lifetime with local abrasion, for 7 strand aramid

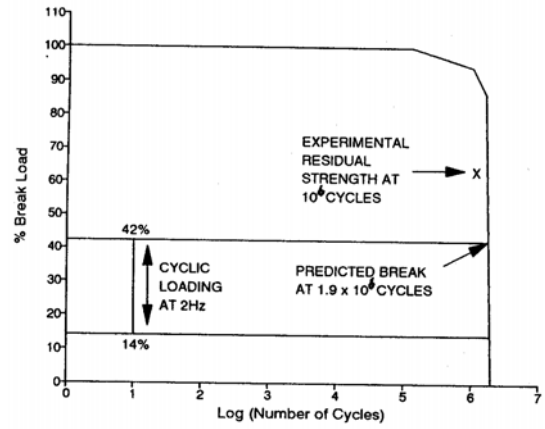

Figure 8. Example of predicted residual lifetime, with global abrasion for aramid wire rope construction

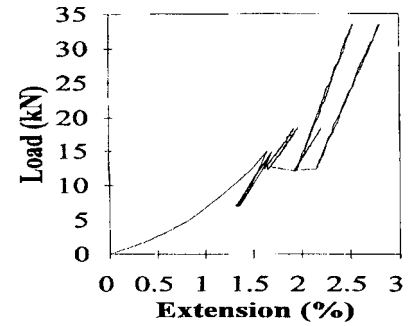

Figure 9. Load-elongation response of a 50kN break load aramid rope showing changes in stiffness and small hysteresis

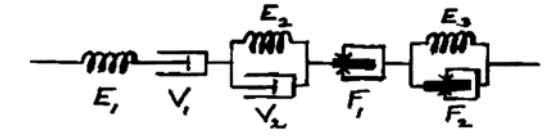

Figure 10. General model for load-deformation response